A Hybrid Photovoltaic-Fuel Cell-Based Single-Stage Grid Integration With Lyapunov Control Scheme

Priyadarshi, Neeraj; Sanjeevikumar, Padmanaban; Bhaskar, Sagar Mahajan; Blaabjerg, Frede; Holm-Nielsen, Jens Bo; Azam, Farooque; Sharma, Amarjeet

Published in:
I E E E Systems Journal

DOI (link to publication from Publisher):
10.1109/JSYST.2019.2948899

Publication date:
2020

Document Version
Accepted author manuscript, peer reviewed version

This article has been accepted for inclusion in a future issue of this journal. Content is final as presented, with the exception of pagination.

A Hybrid Photovoltaic-Fuel Cell-Based Single-Stage Grid Integration With Lyapunov Control Scheme

Neeraj Priyadarshi, Sanjeevikumar Padmanaban, *Senior Member, IEEE*, Mahajan Sagar Bhaskar, *Member, IEEE*, Frede Blaabjerg, *Fellow, IEEE*, Jens Bo Holm-Nielsen, Farooque Azam, and Amarjeet Kumar Sharma

Abstract*—This article presents a single-stage hybrid photovoltaic (PV)-fuel cell (FC)-based grid-integrated system with Lyapunov function-based controller design to obtain optimal power extraction from hybrid renewable sources without maximum power point tracking (MPPT) application. The proposed Lyapunov controller performs MPPT function, improves power quality, and forces inverter to inject sinusoidal current to the utility grid. In this proposed approach, the higher switching frequency has been reduced by employing *LCL* filter inclusion compared to the two-stage hybrid power system. This proposed single-stage system has low cost and improved power quality at the point of common coupling and employed controller injects stable power to the utility grid. In this article, a hybrid overall distributed-particle swarm optimization-based MPPT is employed with FCs and integrated CUK converter. The effectiveness of the employed Lyapunov function-based controller has been tested with dSPACE (DS1104) real-time platform for single-stage hybrid grid-connected power system under varying operating conditions that have high efficiency, reduced harmonic distortion in grid current with the simpler employed power converter. Experimental responses confirm the effectiveness of the proposed controller, which transfers the hybrid power from PV and FC to the utility grid through a single stage.

***Index Terms*—Fuel cell (FC), grid integrated system, Lyapunov function, maximum power point tracking (MPPT), photovoltaic (PV), utility grid.**

I. Introduction

FOSSIL fuels are used to provide electrical power near to the particular load. Thus, an alternative source of power is needed to provide electrical power when loads are situated in remote places. Nowadays, renewable energy sources are an efficient alternative solution to the above issues [1]. The power generations from the photovoltaic generator (PVG) are dependent on solar insolation and ambient temperature [2]. The intermittent nature of renewable energy sources motivated the researchers to use hybrid power system, which provides solutions to variability issues and has higher efficiency with the alternate option without battery system. In order to extract electrical power from hybrid renewable energy sources and injection to load/grid, a proper conversion system is needed which comprise two stage and single-stage conversion system [3]. Compared to double (two) stage power system, the single-stage power conversion systems are more reliable, has lower losses, economical operation, simpler implementation, and has reduced size [4], [5]. The single-stage power conversion system performs double-stage transformation in a single step by doing maximum power point tracking (MPPT) function [6], [7]. In [8], the PVG system has been discussed with sliding mode and Lyapunov function controller for two-stage PV power system as a MPPT and inverter control, respectively. This article deals the active/reactive power grid injection, balanced/unbalanced loading conditions and harmonic reduction with unity power coefficients under different operating conditions. However, due to double-stage grid integration, the stability analysis of grid PV power system has more complexities because of system parameters adjustments.

In [9] and [10], single-stage grid PV power system has been implemented which provides active/reactive power control with unity power factor and operates PV system at maximum power point (MPP) region under changing operating conditions. In this low-voltage PV power system reference grid voltage has been employed for the generation of the tracked reference current. Nevertheless, unity power factor operation of grid system using PV renewable sources. In [11], single-stage PV grid utility using feedback linearized controller have been discussed for dc-link voltage utilization with dq controller as active and reactive power regulator. However, the integration of hybrid renewable energy sources to the utility grid has been missing in this research work for single-stage power system. In [12], voltage sensor-less PV grid utility with single-stage power conversion have been discussed. In this, one-cycle control without phase locked loop has been employed as inverter control for PV grid utility. The employed PV power system does not need any sensor to sense grid voltage. However, the conventional P&O method has been employed for MPPT control and hybrid renewable sources to grid integration is not presented.

To overcome the above-mentioned drawbacks, solar-fuel cell (FC)-based single-stage grid utility is proposed to minimize the

Manuscript received April 2, 2019; revised August 26, 2019; accepted October 12, 2019. *(Corresponding author: Mahajan Sagar Bhaskar.)*

N. Priyadarshi, S. Padmanaban, M. S. Bhaskar, and J. B. Holm-Nielsen are with the Center for Bioenergy and Green Engineering, Department of Energy Technology, Aalborg University, Esbjerg 6700, Denmark (e-mail: neerajrjd@gmail.com; san@et.aau.dk; sagar25.mahajan@gmail.com; jhn@et.aau.dk).

F. Blaabjerg is with the Center of Reliable Power Electronics (CORPE) Department of Energy Technology, Aalborg University, Aalborg 9100, Denmark (e-mail: fbl@et.aau.dk).

F. Azam is with the School of Computing and Information Technology, REVA University, Bangalore 560064, India (e-mail: farooque53786@gmail.com).

A. K. Sharma is with the Department of Electrical Engineering, Birsa Institute of Technology (Trust), Ranchi 835217, India (e-mail: maxeramar@gmail.com).

Digital Object Identifier 10.1109/JSYST.2019.2948899

This article has been accepted for inclusion in a future issue of this journal. Content is final as presented, with the exception of pagination.

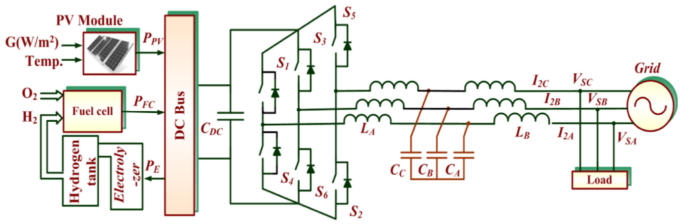

Fig. 1. Overall block diagram of hybrid PV-fuel cell-based single-stage grid integration.

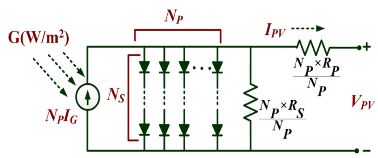

Fig. 2. Basic equivalent PV cell model.

dependency of intermittent behavior of the PV system. The PVG and FC-based hybrid renewable energy sources are integrated to the utility grid with single-stage power conversion system. The PVG works as a primary energy source and provides electrical power to load/grid and surplus power has been employed for the production of H_2 and H_2O. The FC system is treated as a secondary power source and support as an alternative to load/grid requirement whenever PV power generation is deficient. Moreover, Lyapunov-based inverter controller has been proposed which provides MPPT functioning by dc-link voltage regulation as well as unity power factor operation at point of common coupling for grid utility. The newness of this research work is the hybrid PV-FC for single-stage grid utility which is never discussed in the literature using real-time dSPACE board under varying operating conditions.

II. Overall Structure of PV-FC Cell-Based Integration

Fig. 1 depicts a hybrid PV-FC-based single-stage grid integration using Lyapunov function with alkaline water electrolyzer, proton exchanger, and hydrogen tank as major components. PV renewable sources act as main source and extra power has been utilized for the production of hydrogen gas through electrolyzer. Under low solar insolation or higher load power demand, the FC acts like an alternating/supplementary power source.

A. PV Cell Mathematical Modeling

PV modules are designed by combining a number of PV cells in series/parallel connection to achieve high current/voltage to the electrical network. PV modules are formed by the combination of several PV cells which are made by p-n junction principle. The output current of PV module can be calculated by considering basic equivalent circuit of PV cell model [13]. Fig. 2 presents the basic equivalent PV cell model in which *V–I* characteristics governing mathematical relation is

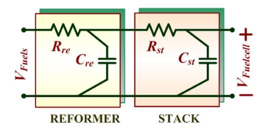

Fig. 3. Equivalent circuit model of fuel cell.

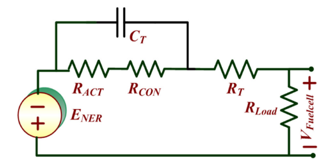

Fig. 4. Basic PEMFC equivalent structure using electrochemical reaction.

described as follows:

$$I_{\mathrm{PV}} = \left(\begin{array}{c} N_P I_G - N_P I_{st}\left(\mathrm{e}^{\left(\frac{Q\left(V_{\mathrm{PV}} + I_{\mathrm{PV}} \cdot R_s \cdot \frac{N_s}{N_P}\right)}{N_s A_D K_B T_K}\right)} - 1 \right) \\ -\frac{\left(\frac{N_P V_{\mathrm{PV}}}{N_s} + I_{\mathrm{PV}} R_s\right)}{R_P} \end{array} \right) \tag{1}$$

where A_D is the diode ideality factor, K_B is the Boltzmann constant, T_K is the Kelvin temperature, Q is a charge on electron, R_S is the series resistance, R_P is the parallel resistance, I_{st} is the Diode saturation constant, and V_{PV}, I_{PV} are output voltage and current of PV, respectively.

B. PEMFC Mathematical Modeling

Fig. 3 depicts the equivalent circuit model of FC comprises reformer and stack unit which is employed to produce electricity with the electrochemical reactions of H_2 and O_2. Mathematically, the transfer functions are expressed using the above equivalent model of the FC as follows:

$$\frac{V_{cre}}{V_{\mathrm{Fuels}}} = \frac{1/C_{re}S}{R_{re} + 1/C_{re}S} = \frac{1}{1 + R_{re}C_{re}S} \tag{2}$$

$$\frac{V_{cst}}{V_{cre}} = \frac{1/C_{st}S}{R_{st} + 1/C_{st}S} = \frac{1}{1 + R_{st}C_{st}S}. \tag{3}$$

Fig. 4 describes the basic PEMFC equivalent structure using electrochemical reaction and mathematical relation governing for designing FC is as follows:

$$E_{\mathrm{NER}} = \left(\begin{array}{c} 1229 \times 10^{-3} - 85 \times 10^{-5} \\ \times (T_c - 298.15) \\ +431 \times 10^{-7} \end{array} \right) \times T_c \left[\begin{array}{c} \ln \ln (P_{H_2}) + \\ \frac{1}{2} \ln \ln (P_{O_2}) \end{array} \right] \tag{4}$$

$$V_{\mathrm{Fuel\ cell}} = E_{\mathrm{NER}} - V_{\mathrm{ACT}} - V_{\mathrm{OHM}} - V_{\mathrm{CON}} \tag{5}$$

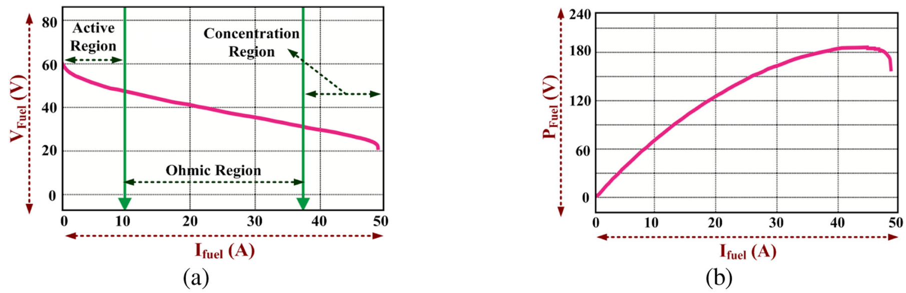

Fig. 5. (a) Voltage/current characteristics of fuel cell classified into activation, ohmic, and concentration regions. (b) Power/current characteristics of fuel cell.

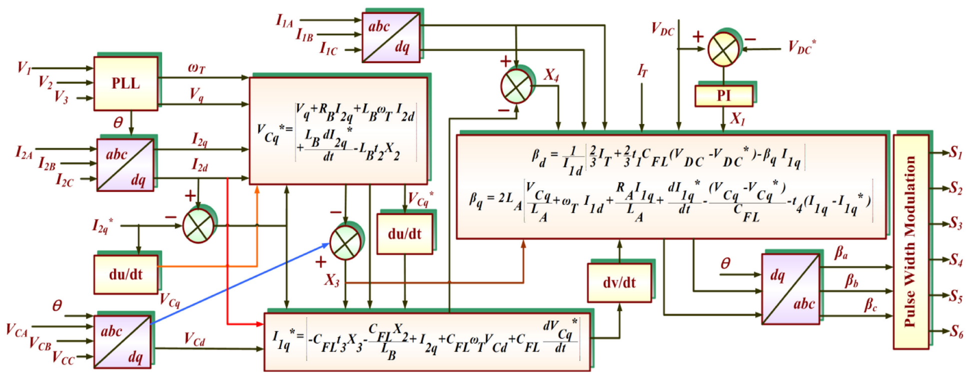

Fig. 6. Lyapunov-based single-stage controller.

$$V_{\mathrm{ACT}} = -[\xi/A + \xi/BT_c + \xi/C \times T_c \times \ln\ln(CO_2)] \quad (6)$$

$$CO_2 = \frac{P_{O_2}}{508 \times 10^4 \times e^{-(498/T_c)}} \quad (7)$$

$$V_{\mathrm{OHM}} = I_{\text{Fuel cell}}\,(R_{MR} + R_{CR}) \quad (8)$$

$$R_{MR} = (\rho_{MR} \times \lambda_M)/A_M \quad (9)$$

$$V_{\mathrm{CON}} = \ln\ln(1 - J_i/J^{\max}) \times (-B_M) \quad (10)$$

where B_M is the parametric FC coefficient, ρ_{MR} is the membrane specific resistivity, λ_M is the membrane thickness, A_M is the active membrane area, T_c is the FC operating temperature, V_{CON} is drop in voltage due to concentration loss, E_{NER} is the Nernst potential, $J_{\max}$ is the peak current density, P_{O2} is the partial pressure of oxygen, P_{H2} is the partial pressure of hydrogen, ξ/A, ξ/B, ξ/C are model coefficients, R_{MR} is the equivalent membrane resistance, and R_{CR} is the equivalent contact resistance.

Fig. 5(a) depicts the voltage/current characteristics of FC which is classified into activation, ohmic, and concentration regions in which FC voltage decreases as FC current increases. Fig. 5(b) presents FC power versus current behavior.

III. Lyapunov Function-Based Inverter Controller

This section explains the employment of Lyapunov function-based control strategy to perform multifunctioning objectives, viz., MPPT, injection of sinusoidal inverter current to the utility grid, and improved power quality at point of common coupling. The MPPT operation is carried out by keeping dc-link voltage constant. It can reduce the higher switched frequency of inserting *LCL* (Passive) filter between inverter and utility grid. The active currents are controlled to inject stable power to utility grid. Fig. 6 depicts the designed block diagram of Lyapunov-based single-stage controller.

A. Mathematical Modeling of 3-ϕ Hybrid Grid Integration

$$C_{\mathrm{DC}}\frac{dV_{\mathrm{DC}}}{dt} = I_T - \frac{3}{2}(\beta_d I_{1d} + \beta_q I_{1q}) \quad (11)$$

$$\left.\begin{aligned} L_A dI_{1d}/dt + R_A I_{1d} &= \beta_d \tfrac{V_{\mathrm{DC}}}{2} - V_{Cd} + \omega_T L_A I_{1q} \\ L_A dI_{1q}/dt + R_A I_{1q} &= \beta_d \tfrac{V_{\mathrm{DC}}}{2} - V_{Cq} - \omega_T L_A I_{1d} \end{aligned}\right\} \quad (12)$$

$$\left.\begin{aligned} L_B dI_{2d}/dt + R_B I_{2d} &= V_{Cd} - V_d + \omega_T L_A I_{2q} \\ L_B dI_{2q}/dt + R_B I_{2q} &= V_{Cq} - V_q + \omega_T L_A I_{2d} \end{aligned}\right\} \quad (13)$$

$$\left.\begin{aligned} C_{FL} dV_{Cd}/dt &= I_{1d} - I_{2d} + \omega_T C_{FL} V_{Cq} \\ C_{FL} dV_{Cq}/dt &= I_{1q} - I_{2q} + \omega_T C_{FL} V_{Cd} \end{aligned}\right\} \quad (14)$$

where C_{DC} is the dc-link capacitor, L_A, R_A is the equivalent inductance and resistance at inverter portion, L_B, R_B is the equivalent inductance and resistance at grid portion, C_{FL} is the capacitance of filter, V_{Cd}, V_{Cq} are synchronous *dq* reference (voltage across filter capacitor), I_{1d}, I_{1q} is the synchronous *dq* reference (current through inverter), I_{2d}, I_{2q} is the synchronous *dq* reference (current through filter), V_d, V_q is the synchronous *dq* reference (voltage across grid), ω_T is the synchronous *dq* reference (angular grid frequency), β_d, β_q is the synchronous *dq* reference frame (control rules).

The error in dc-link voltage is defined as one state variable as follows:

$$X_1 = V_{\rm DC} - V_{\rm DC}^* \tag{15}$$

where $V_{\rm DC}{}^*$ is the reference dc-link voltage. Also, the $\dot{X}_1$ can be expressed mathematically as follows:

$$\dot{X}_1 = \frac{1}{C_{FL}}\left[I_T - \frac{3}{2}\left(\beta_d I_{1d} + \beta_q I_{1q}\right)\right]. \tag{16}$$

The proposed controller forces the grid current to become sinusoidal and in phase with grid voltage. Moreover, using the synchronous *dq* reference frame, the active ($P_{\rm act}$) and reactive ($Q_{\rm rec}$) power supplied to utility grid can be described mathematically as follows:

$$\left.\begin{array}{l} P_{\rm act} = \frac{3}{2}\left(V_d I_d + V_q I_q\right) \\ Q_{\rm rec} = \frac{3}{2}\left(V_q I_d - V_d I_q\right) \end{array}\right\}. \tag{17}$$

The reactive power $Q_{\rm rec}$ can be controlled by regulating I_q with keeping V_d constant and V_q becomes zero with frame of synchronous *dq* reference, i.e., $Q_{\rm rec} = 1.5(V_q I_d - V_d I_q)$. Therefore, I_q current is regulated with $I_{2q}*$ reference current is 0. Another state variable is assigned to error produced in filter current and expressed mathematically as follows:

$$\dot{X}_2 = I_{2q} - I_{2q}^*. \tag{18}$$

Also

$$\dot{X}_2 = -R_B I_{2q}/L_B + \frac{V_{Cq}}{L_B} - \frac{V_q}{L_B}\omega_T I_{2d} - \frac{dI_{2q}^*}{dt}. \tag{19}$$

The Lyapunov controller has been employed to reduce the system complexities which provides reduced (zero) errors in state variables under transient operating conditions. Mathematically, the system overall saving energy can be denoted as follows:

$$V_E\left(X\right) = \frac{1}{2}\left[X_1^2 + X_2^2\right]. \tag{20}$$

The system becomes global stable whenever $V_E(X) < 0$, $\forall X$ and $t_i > 1$ makes the system global asymptotic stability

$$\dot{X}_1 = -t_1 X_1 \tag{21}$$

$$\dot{X}_2 = -t_2 X_2. \tag{22}$$

By combining (16) and (21), (19 and (22), one can obtain

$$\frac{1}{C_{FL}}\left[I_T - \frac{3}{2}\left(\beta_d I_{1d} + \beta_q I_{1q}\right)\right] = t_1 X_1 \tag{23}$$

$$-R_B I_{2q}/L_B + \frac{V_{Cq}}{L_B} - \frac{V_q}{L_B}\omega_T I_{2d} - \frac{dI_{2q}^*}{dt} = t_2 X_2. \tag{24}$$

Considering V_{Cq} as a virtual controlling parameter, the reference voltage across filter capacitor is expressed as follows:

$$V_{Cq}^* = V_q + R_B I_{2q} + L_B \omega_T I_{2d} + L_B \frac{dI_{2q}^*}{dt} - L_B t_2 X_2. \tag{25}$$

Additionally, the third state variable is defined as follows:

$$X_3 = V_{Cq} - V_{Cq}^*. \tag{26}$$

By combining (19) and (26), one can obtain

$$\dot{X}_2 = \frac{X_3}{L_B} - t_2 X_2 \tag{27}$$

Mathematically, modified Lyapunov function becomes

$$V_{E_1}\left(x\right) = V_E(x) + \frac{1}{2}X_3^2. \tag{28}$$

Also

$$\dot{X}_3 = \frac{I_{1q}}{C_{FL}} - \frac{I_{2q}}{C_{FL}} - \omega_T V_{CD} - \frac{dV_{Cq}^*}{dt}. \tag{29}$$

By calculation

$$\dot{V}_E\left(x\right) = -t_1 X_1^2 - t_2 X_2^2 + X_3\left(\dot{X}_3 + \frac{X_2}{L_B}\right). \tag{30}$$

Ensuring modified Lyapunov strategy, the assumption is

$$\dot{X}_3 + \frac{X_2}{L_B} = -t_3 X_3. \tag{31}$$

By combining (29) and (31), one can obtain the following:

$$\frac{I_{1q}}{C_{FL}} - \frac{I_{2q}}{C_{FL}} - \omega_T V_{CD} - \frac{dV_{Cq}^*}{dt} + \frac{X_2}{L_B} = -t_3 X_3. \tag{32}$$

The stabilized function can be evaluated by assigning I_{1q} as virtual controlling parameters

$$I_{1q}^* = \begin{pmatrix} -C_{FL} t_3 X_3 - C_{FL}\frac{X_2}{L_B} \\ +I_{2q} + C_{FL}\omega_T V_{CD} + C_{FL}\frac{dV_{Cq}^*}{dt} \end{pmatrix}. \tag{33}$$

Considering error produced by current through filter as fourth state variable is expressed mathematically as follows:

$$X_4 = I_{1q} - I_{1q}^*. \tag{34}$$

By combining (29) and (34), one can obtain

$$\dot{X}_3 = \frac{X_4}{C_{FL}} - t_3 X_3 - \frac{X_2}{L_B}. \tag{35}$$

The Global Lyapunov function has been expressed as follows:

$$V_{EG}\left(X\right) = V_{E_1}\left(x\right) + \frac{1}{2}X_4^2. \tag{36}$$

By solving the above

$$\dot{V}_{EG}\left(X\right) = -t_1 X_1^2 - t_2 X_2^2 - t_3 X_3^2 + X_4\left(\dot{X}_4 + \frac{X_3}{C_{FL}}\right). \tag{37}$$

Assuming global Lyapunov stability

$$\dot{X}_4 + \frac{X_3}{C_{FL}} = -t_4 X_4 \tag{38}$$

$$\dot{V}_{EG}\left(X\right) = -t_1 X_1^2 - t_2 X_2^2 - t_3 X_3^2 - t_4 X_4^2 < 0. \tag{39}$$

Equation (39) reveals that the overall system becomes globally stabilized only when $\dot{V}_{EG}(X)$should be negative.

On substituting, error dynamics in (38), one can obtain the following:

$$\beta_q \frac{V_{\mathrm{DC}}}{2L_A} - \frac{V_{Cq}}{L_A} - \omega_T I_{1d} - \frac{R_A I_{1q}}{L_A} - \frac{dI_{1q}^*}{dt} + \frac{X_3}{C_{FL}} = -t_4 X_4. \tag{40}$$

Combining (33) and (40) to achieve control variables to track reference $V_{\mathrm{DC}}*$ and obtain unit power coefficients

$$\begin{bmatrix} \beta_d \\ \beta_q \end{bmatrix} = \begin{bmatrix} \frac{3}{2} I_{1d} & \frac{3}{2} I_{1q} \\ 0 & \frac{V_{\mathrm{DC}}}{2L_A} \end{bmatrix} \begin{bmatrix} I_T + \frac{2}{3} t_1 C_{FL} X_1 \\ \left(\begin{matrix} \frac{V_{Cq}}{L_A} + \omega_T I_{1d} + \frac{R_A I_{1q}}{L_A} \\ + \frac{dI_{1q}^*}{dt} - \frac{X_3}{C_{FL}} - t_4 X_4 \end{matrix} \right) \end{bmatrix}. \tag{41}$$

The active/reactive power has been controlled through *d/q* components and tracking error can be calculated as follows:

$$E_d(T) = I_{d\mathrm{ref}} - I_d \tag{42}$$

$$E_q(T) = I_{q\mathrm{ref}} - I_q. \tag{43}$$

$I_{q\mathrm{ref}}$ has been forced to become zero for obtaining unity power factor operation. The proposed inverter is controlled such that the inverter current follows the corresponding references to maintain grid current pulse sinusoidally and also to ensure reactive power zero. The *p–q* theory is employed to evaluate the current reference which facilitates the minimization of dc-link ripples [14].

The current reference is evaluated mathematically as (for one phase)

$$I_{C\mathrm{ref}} = I_{\mathrm{load}} - I_{\mathrm{gridcurrent}}. \tag{44}$$

IV. OD-PSO-Based MPPT for Fuel Cell

In equated with classical MPPT algorithms, the intelligent MPPT methods are able to find global MPP under fluctuating weather conditions with low computational burden and cost. Because of simpler mathematical analysis, the particle swarm optimization (PSO) has been used widely. However, nonconvergence and problems to achieve global MPP (GMPP) are the major drawbacks of PSO-based MPPT method. As far as intelligent MPPT methods implementation through particle setup is concerned, the initial parameter is required to evaluate GMPP. Moreover, values of open-circuit voltage and short current needed to find GMPP which minimizes the feasibility of hardware implementation of these algorithms.

To overcome the shortcomings of intelligent optimized MPPT methods, in this article, a hybrid overall distributed-particle swarm optimization (OD-PSO)-based MPPT is proposed which do not need information related to hardware specifications and able to obtain GMPP under varying weather conditions with accurate and rapid responses [15]. The overall distributed method-based MPPT provides neighborhood locality of GMPP which simplify the initial parameter and drifted to PSO method. After initializing the parameter, the PSO method is able to achieve exact GMPP region, rapidly. Kennedy and Eberhart has introduced PSO algorithm. In this article, a hybrid OD-PSO-based MPPT

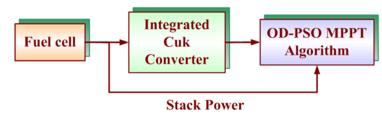

Fig. 7. OD-PSO-based MPPT for fuel cell.

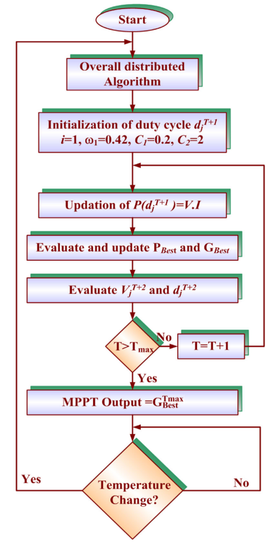

Fig. 8. Flowchart of OD-PSO-based MPPT for fuel cell.

has been employed with FC and integrated CUK converter as show in Fig. 7 [16]. The overall distributed method provides rapid searching of region nearer to GMPP.

Mathematically, PSO algorithm is expressed as follows:

$$V_j^{T+1} = \omega_i V_j^T + C_1 R_2 \left(P_{\mathrm{Best}j} - X_j^T \right) + C_2 R_3 \left(G_{\mathrm{Best}j} - X_j^T \right) \tag{45}$$

$$X_j^{T+1} = X_j^T + V_j^{T+1} \tag{46}$$

where T is the number of iteration, ω_I is the weight of inertia, R_2 and R_3 are random parameters in [0,1], C_1 and C_2 are cognitive and social coefficients, V_j^T is the offset position vector at the Tth iteration, X_j^T is position of particle at the Tth iteration, $P_{\mathrm{Best}j}, G_{\mathrm{Best}j}$ are Personal and Global best position of particle, respectively.

The overall distributed algorithm provides the searching of particles in a trivial area containing GMPP. And achieved particles are employed as an antecedent fragment for PSO method and GMPP region can be located and presented using flow chart in Fig. 8.

V. Hardware Prototype and Experimental Results

The feasibility and effectiveness of the proposed Lyapunov control scheme has been tested for PV-FC-based single-stage hybrid grid integration system under varying operating conditions using dSPACE1104 real-time control board. The responses obtained through simulation (MATLAB/Simulink) have been

This article has been accepted for inclusion in a future issue of this journal. Content is final as presented, with the exception of pagination.

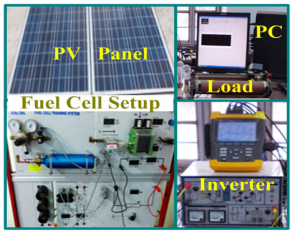

Fig. 9. Lyapunov-based single-stage PV-fuel system.

TABLE I
DESIGN PARAMETERS

Parameters	Value
PV rated voltage	25 V
PV rated current	8 A
Grid Voltage	230 V
Grid current	30 A
Fuel cell rated voltage	25 V
Fuel cell rated current	8 A
Type of Electrolyte	Alkaline
Anode/ cathode coeff. of transfer	0.3, 0.5
Electrolyzer temperature	50^0 C

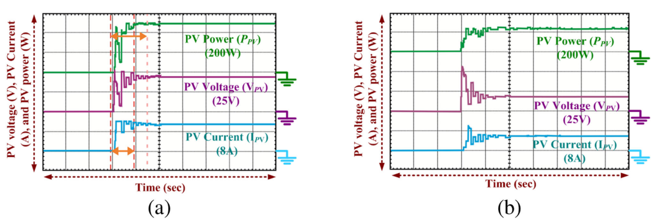

Fig. 10. PV tracking power under (a) uniform solar insolation level and (b) partial shading conditions.

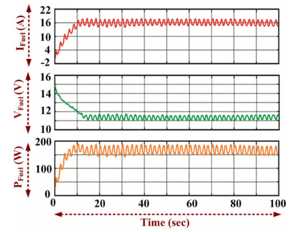

Fig. 11. Fuel cell MPPT operation.

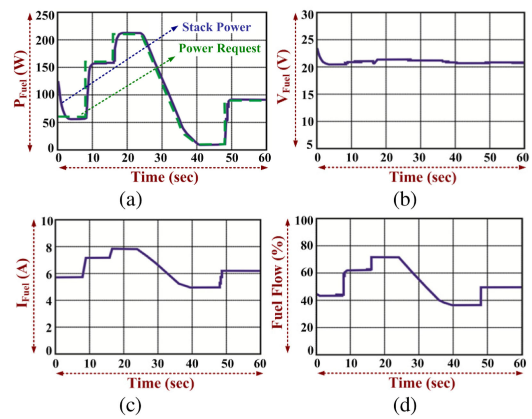

Fig. 12. Practical responses of fuel cell extracted optimum fuel cell flow rate, fuel cell voltage, fuel cell current and extracted fuel cell power using the proposed MPP controller.

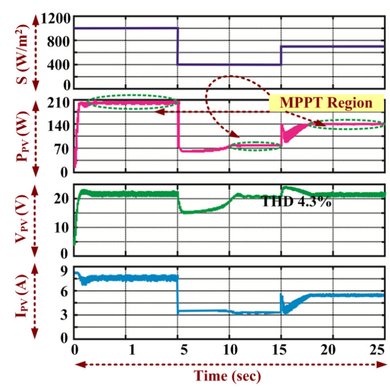

Fig. 13. Practical responses of fuel cell MPPT operation of the proposed PV system at different sun insolation level.

tested practically by developing 200 W hybrid PV-FC grid integrated power system. Inverter switching pulses have been generated using dSPACE interface which is fed to opto-coupler for isolation purpose. DSP-dSPACE (1104) interface comprises ADC and DAC converters with FLUKE43B power quality analyzer as well as digital storage oscilloscope have been employed to measure signals under varying operating conditions. Control desk platform has been employed to monitor FC voltage/current and received signals are fed to the data acquisition system through Heliocentric which are implemented using dSPACE DS1104 real-time interface. In this experiment for the measurement of FC current, ACS712ELCTR-30-A-T as a hall sensor (66 mV/A precision and 30A range) with IRFZ24N MOSFET as switching component has been employed. Fig. 9 describes the experimental set up of hybrid PV-FC-based single-stage grid integration. Table I describes the employed design parameters for implementation of the proposed hybrid power system. Experimental response presented in Fig. 10(a) reveals that PV power tracking has been achieved with accurate MPP region under uniform solar insolation level. Moreover, Fig. 10(b) presents the accurate PV power tracking under partial shading conditions with accurate MPPT achievement. The practical responses presented in Fig. 11 depicts that the FC current reached to MPP region and having magnitude 8 A at $t = 10$ s, while FC voltage has reached to 25 V and maximum FC extracted power with 200 W has been obtained. The obtained practical results closely matched with FC modeling estimated values. Fig. 12 presents the practical responses of FC extracted optimum FC flow rate, FC voltage, FC current and extracted FC power using the proposed MPP controller. The peak power from FC has been extracted under varying FC flow rate. The MPPT operation of the proposed PV system has been evaluated at different sun insolation level and presented using Fig. 13. From $t = 0$ to $t = 5$ s, the sun insolation level is kept 1000 W/m^2. Moreover, at $t = 5$ s to $t = 15$ s, the solar irradiance level is maintained at 400 W/m^2 and again it is increased to 600 W/m^2 upto $t = 25$ s. The PV maximum power has been extracted and MPP is obtained under

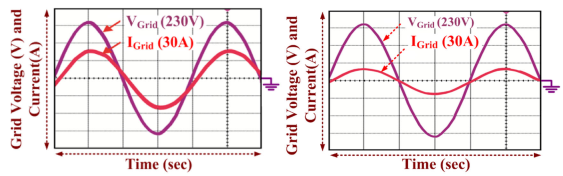

(a) (b)

Fig. 14. Practically found grid voltage and current responses at solar irradiance level. (a) $G = 1000$ W/m^2. (b) 500 W/m^2.

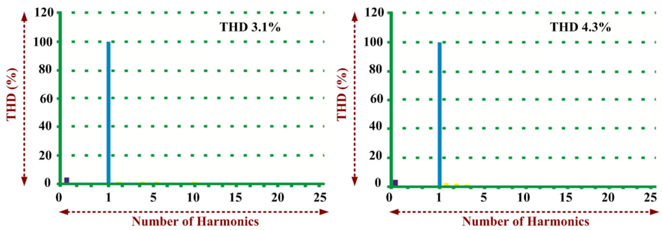

(a) (b)

Fig. 15. Total harmonic distortion present in grid current at solar irradiance level using the conventional fuzzy-PI controller. (a) 1000 W/m^2. (b) 500 W/m^2.

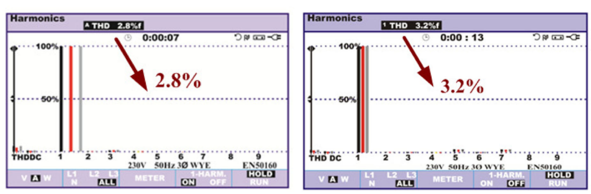

(a) (b)

Fig. 16. Total harmonic distortion present in grid current at solar irradiance level using the proposed Lyapunov controller. (a) 1000 W/m^2. (b) 500 W/m^2.

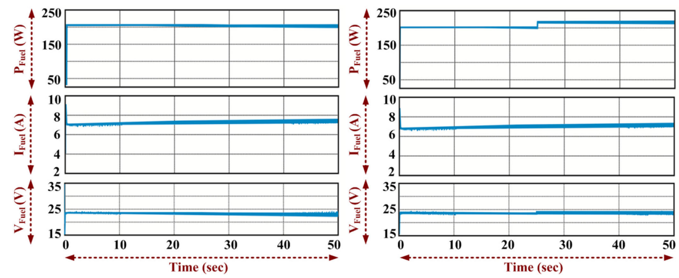

(a) (b)

Fig. 17. Performance of the fuel MPPT under (a) steady state and (b) dynamic operating conditions.

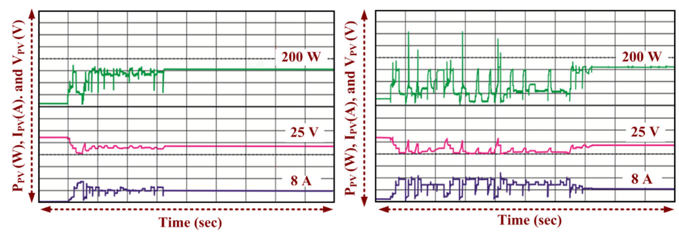

(a) (b)

Fig. 18. Performance of the PV system using (a) Lyapunov controller and (b) conventional fuzzy-PI controller.

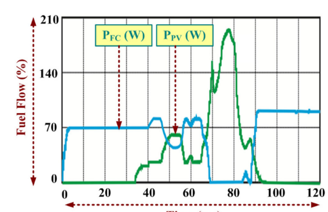

Fig. 19. Obtained PV and fuel cell power.

each operating conditions with reduced ripple in PV system responses. Experimental results reveal that MPP operation is achieved at different sun irradiance level.

Practically found grid voltage and current responses confirm that extracted PV and FC power is fed to the utility grid effectively and measured by 3034 A (Agilent oscilloscope) at G is 1000 and 500 W/m^2 solar irradiance level and presented by Fig. 14(a) and (b). Moreover, with the FLUKE (Power quality analyzer) the total harmonic distortion present in grid current have been achieved as 3.1% and 4.3%, respectively, using conventional fuzzy-PI controller and presented by Fig. 15(a) and (b). While THD of grid current is found 2.8% and 3.2%, respectively, at the same operating conditions depicted in Fig. 16(a) and (b). Experimentally obtained total harmonic distortion of grid current is within IEEE 519 standard and PV module tries to fed I_{PV} to the utility grid with reduced THD. The total harmonics of grid current using the proposed Lyapunov controller has been calculated experimentally. Fig. 16(a) and (b) represent the THD of grid current at solar irradiance of 1000 and 500 W/m^2, respectively. The practical results presented in Fig. 17(a) and (b) demonstrate the performance of the proposed controller under steady-state and dynamic operating conditions, respectively. During transient operation, the performance of the hybrid power system has been evaluated when solar irradiance level varies from 500 to 1000 W/m^2. Fig. 17(b) reveals that the dynamic performance of the proposed controller is found satisfactory during step variation of sun irradiance level and I_{PV} is found to operate under MPP region. Experimental results of FC responses under step variation of solar insolation, which reveals that the proposed MPPT controller forces FC to work under MPP region under changing environmental temperature. The MPPT performance of the single-stage PV power system is realized with the proposed and conventional controllers. Fig. 18(a) reveals the tracking of GMPP tracking under partial shading conditions with precise and accurate responses, while Fig. 18(b) explains the behavior of PV power system using conventional control under partial shade conditions and global maximum power is obtained with oscillation nearer to MPP.

Fig. 19 presents obtain PV and FC power and surplus power has been employed for the generation of hydrogen gas applied has been described using Fig. 20 to water electrolysis. Lyapunov inverter controller response parameters are tabulated in Table II. The behavior of the proposed Lyapunov-based inverter controller has been compared with classical PI controller.

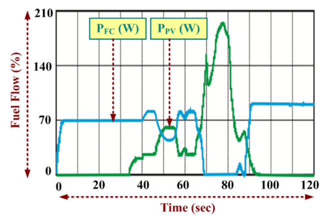

Fig. 20. Surplus for generation of hydrogen gas using an electrolyzer.

TABLE II
RESPONSE PARAMETERS OF LYAPUNOV INVERTER CONTROLLER

Parameters	Specifications
Rise Time	70 ms
Peak overshoot	5×10^{-2} %
Setting Period	105 ms
Steady state error	2.5×10^{-1} V

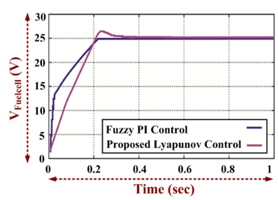

Fig. 21. Lyapunov versus fuzzy–PI controller.

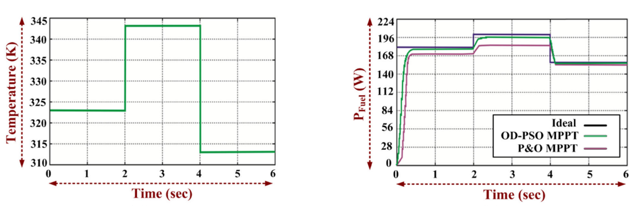

(a) (b)

Fig. 22. OD-PSO versus P&O based MPPT for fuel cell under varying temperature. (a) Change in temperature. (b) Change in fuel cell power.

Fig. 21 reveals that using the proposed Lyapunov controller, the output voltage reaches the reference value more precisely compared to conventional fuzzy-PI controller and has better peak overshoot and steady-state error. Fig. 22 demonstrates the performances of FC-based MPPT under varying temperature with proposed OD-PSO and perturb and observe [17] based MPPT techniques.

VI. CONCLUSION

The Lyapunov-based control strategy for single-stage grid integration is presented for hybrid PV-FC-based power system. In the proposed scheme, PVG has been worked as primary and FC as secondary renewable energy sources in which power generated from PV sources employed for load/grid requirement and surplus power has been utilized to generate H_2 using electrolysis of H_2O. Experimental results demonstrate that the proposed hybrid PV-FC-based single-stage grid power system injected hybrid renewable sources power to utility grid accurately and operated near to MPP region effectively. Practical responses confirm the effective performance of the single-stage hybrid grid power system which has reduced switch losses, higher performance gain with economical and simpler design implementation.

REFERENCES

[1] N. Priyadarshi, S. Padmanaban, P. K. Maroti, and A. Sharma, "An extensive practical investigation of FPSO-based MPPT for grid integrated PV system under variable operating conditions with anti-islanding protection," *IEEE Syst. J.*, vol. 13, no. 2, pp. 1861–1871, Jun. 2019.

[2] N. Priyadarshi, S. Padmanaban, M. S. Bhaskar, F. Blaabjerg, and A. Sharma, "Fuzzy SVPWM-based inverter control realisation of grid integrated photovoltaic-wind system with fuzzy particle swarm optimisation maximum power point tracking algorithm for a grid-connected PV/wind power generation system: Hardware implementation," *IET Elect. Power Appl.*, vol. 12, no. 7, pp. 962–971, Apr. 2018.

[3] B. N. Alajmi, K. H. Ahmed, G. P. Adam, and B. W. Williams, "Single-phase single-stage transformer less grid-connected PV system," *IEEE Trans. Power Electron.*, vol. 28, no. 6, pp. 2664–2676, Jun. 2013.

[4] M. A. Herran, J. R. Fischer, S. A. Gonzalez, M. G. Judewicz, and D. O. Carrica, "Adaptive dead-time compensation for grid-connected PWM inverters of single-stage PV systems," *IEEE Trans. Power Electron.*, vol. 28, no. 6, pp. 2816–2825, Jun. 2013.

[5] P. Cossutta, M. P. Aguirre, A. Cao, S. Raffo, and M. I. Valla, "Single-stage fuel cell to grid interface with multilevel current-source inverters," *IEEE Trans. Ind. Electron.*, vol. 62, no. 8, pp. 5256–5264, Aug. 2015.

[6] A. Kumar and V. Verma, "Performance enhancement of single-phase grid-connected PV system under partial shading using cascaded multilevel converter," *IEEE Trans. Ind. Appl.*, vol. 54, no. 3, pp. 2665–2676, May 2018.

[7] F. Lin, K. Lu, and B. Yang, "Recurrent fuzzy cerebellar model articulation neural network based power control of a single-stage three-phase grid-connected photovoltaic system during grid faults," *IEEE Trans. Ind. Electron.*, vol. 64, no. 2, pp. 1258–1268, Feb. 2017.

[8] M. Rezkallah, S. K. Sharma, A. Chandra, B. Singh, and D. R. Rousse, "Lyapunov function and sliding mode control approach for the solar-PV grid interface system," *IEEE Trans. Ind. Electron.*, vol. 64, no. 1, pp. 785–795, Jan. 2017.

[9] T. Sreekanth, N. Lakshminarasamma, and M. K. Mishra, "A single-stage grid-connected high gain buck–boost inverter with maximum power point tracking," *IEEE Trans. Energy Convers.*, vol. 32, no. 1, pp. 330–339, Mar. 2017.

[10] T. Sreekanth, N. Lakshminarasamma, and M. K. Mishra, "Grid tied single-stage inverter for low-voltage PV systems with reactive power control," *IET Power Electron.*, vol. 11, no. 11, pp. 1766–1773, Apr. 2018.

[11] V. N. Lal and S. N. Singh, "Control and performance analysis of a single-stage utility-scale grid-connected PV system," *IEEE Syst. J.*, vol. 11, no. 3, pp. 1601–1611, Sep. 2017.

[12] E. S. Sreeraj, K. Chatterjee, and S. Bandyopadhyay, "One-cycle-controlled single-stage single-phase voltage-sensorless grid-connected PV system," *IEEE Trans. Ind. Electron.*, vol. 60, no. 3, pp. 1216–1224, Mar. 2013.

[13] K. Moutaki, H. Ikaouassen, A. Raddaoui, M. Rezkallah, and A. Chandra, "Improved lyapunov function based approach for single stage inverter interfacing solar photovoltaic system," in *Proc. Int. Conf. Ind. Technol.*, Apr. 2018, pp. 1000–1005.

[14] S. Dasgupta, S. N. Mohan, S. K. Sahoo, and S. K. Panda, "Lyapunov function-based current controller to control active and reactive power flow from a renewable energy source to a generalized three-phase microgrid system," *IEEE Trans. Ind. Electron.*, vol. 60, no. 2, pp. 799–813, Feb. 2013.

[15] H. Li, D. Yang, W. Su, J. Lü, and X. Yu, "An overall distribution particle swarm optimization MPPT algorithm for photovoltaic system under partial shading," *IEEE Trans. Ind. Electron.*, vol. 66, no. 1, pp. 265–275, Jan. 2019.

[16] S. Padmanaban, N. Priyadarshi, M. S. Bhaskar, J. B. Holm-Nielsen, E. Hossain, and F. Azam, "A hybrid photovoltaic-fuel cell for grid integration with Jaya-based maximum power point tracking: Experimental performance evaluation," *IEEE Access*, vol. 7, pp. 82978–82990, 2019.

[17] S. Padmanaban *et al.*, "A novel modified sine-cosine optimized MPPT algorithm for grid integrated PV system under real operating conditions," *IEEE Access*, vol. 7, pp. 10467–10477, 2019.

Neeraj Priyadarshi received the M.Tech. degree in power electronics and drives from the Vellore Institute of Technology (VIT), Vellore, India, in 2010, and the Ph.D. degree from the Government College of Technology and Engineering, Udaipur, India.

He is currently an external Postdoctoral Researcher with the Department of Energy Technology, Aalborg University, Esbjerg, Denmark. He was with the MIT, Purnea, India, JK University, Geetanjali Institute, Global Institute, and SS Group, Rajasthan, India. He has authored or coauthored more than 40 papers in journals and conferences. His current research interests include power electronics, control system, power quality, and solar power generation.

Dr. Priyadarshi is a Reviewer of *International Journal of Renewable Energy Research.*

Sanjeevikumar Padmanaban (M'12–SM'15) received the bachelor's degree in electrical engineering from the University of Madras, Chennai, India, in 2002, the master's (Hons.) degree in electrical engineering from Pondicherry University, Puducherry, India, in 2006, and the Ph.D. degree in electrical engineering from the University of Bologna, Bologna, Italy, in 2012.

He was an Associate Professor with VIT University from 2012 to 2013. In 2013, he joined the National Institute of Technology, India, as a faculty member. In 2014, he was invited as a Visiting Researcher at the Department of Electrical Engineering, Qatar University, Doha, Qatar, funded by the Qatar National Research Foundation (Government of Qatar). He continued his research activities with the Dublin Institute of Technology, Dublin, Ireland, in 2014. He was an Associate Professor with the Department of Electrical and Electronics Engineering, University of Johannesburg, Johannesburg, South Africa, from 2016 to 2018. Since 2018, he has been a faculty member with the Department of Energy Technology, Aalborg University, Esbjerg, Denmark. He has authored more than 300 scientific papers.

He was the recipient of the Best Paper cum Most Excellence Research Paper Award from IETSEISCON'13, IET-CEAT'16, IEEE-EECSI'19, IEEE-CENCON'19 and five best paper awards from ETAEERE'16 sponsored Lecture Notes in Electrical Engineering, Springer book. He is a Fellow of the Institution of Engineers, India, the Institution of Electronics and Telecommunication Engineers, India, and the Institution of Engineering and Technology, U.K. He is an Editor/Associate Editor/Editorial Board for refereed journals, in particular the IEEE SYSTEMS JOURNAL, IEEE ACCESS, *IET Power Electronics*, and *Journal of Power Electronics* (Korea), and the Subject Editor for the *IET Renewable Power Generation, IET Generation, Transmission and Distribution*, and *FACTS* journal (Canada).

Mahajan Sagar Bhaskar (M'15) received the bachelor's degree in electronics and telecommunication engineering from the University of Mumbai, Mumbai, India, in 2011, and the master.s degree in power electronics and drives from the Vellore Institute of Technology, VIT University, Vellore, India in 2014, and the Ph.D. degree in electrical and electronic engineering, University of Johannesburg, Johannesburg, South Africa, in 2019.

He is currently an external Postdoctoral Researcher with the Department of Energy Technology, Aalborg University, Esbjerg, Denmark. He was a Researcher Assistant with the Department of Electrical Engineering, Qatar University, Doha, Qatar. He was as an Assistant Professor and Research Coordinator with the Department of Electrical and Electronics Engineering, Marathwada Institute of Technology (MIT), Aurangabad, India. He has authored more than 100 scientific papers. He is a reviewer of various international journals and conferences including IEEE and IET. He has authored/coauthored scientific papers in the field of power electronics, with particular reference to XY converter family, multilevel dc/dc and dc/ac converter, and high-gain converter.

Dr. Bhaskar was the recipient of Best Research Paper Awards from IEEE ICCPCT'14, IET-CEAT'16, IEEE-CENCON'19, ETAEERE'16 sponsored Lecture Note in Electrical Engineering, Springer book series, and the IEEE ACCESS AWARD "Reviewer of Month" in January 2019 for his valuable and thorough feedback on manuscripts, and for his quick turnaround on reviews. He is a member of IEEE Industrial Electronics, IEEE Power Electronics, IEEE Industrial Application, IEEE Power and Energy, IEEE Robotics and Automation, IEEE Vehicular Technology Societies, Young Professionals, and various IEEE Technical Councils and Communities.

Frede Blaabjerg (S'86–M'88–SM'97–F'03) received the Ph.D. degree in electrical engineering from Aalborg University, Aalborg, Denmark, in 1995.

He was with ABB-Scandia, Randers, Denmark, from 1987 to 1988. From 1988 to 1992, he was with Aalborg University. He was an Assistant Professor in 1992, an Associate Professor in 1996, and a Full Professor in power electronics and drives in 1998. Since 2017, he has been a Villum Investigator. He is an honoris causa with University Politehnica Timisoara, Romania, and Tallinn Technical University, Estonia. He has authored or coauthored more than 600 journal papers in the fields of power electronics and its applications. He is the coauthor of four monographs and editor of ten books in power electronics and its applications. His current research interests include power electronics and its applications, such as in wind turbines, PV systems, reliability, harmonics, and adjustable speed drives.

Dr. Blaabjerg was the recipient of the 30 IEEE Prize Paper Awards, the IEEE PELS Distinguished Service Award in 2009, the EPE-PEMC Council Award in 2010, the IEEE William E. Newell Power Electronics Award 2014, and the Villum Kann Rasmussen Research Award 2014. He was the Editor-in-Chief of the IEEE TRANSACTIONS ON POWER ELECTRONICS from 2006 to 2012. He was a Distinguished Lecturer for the IEEE Power Electronics Society from 2005 to 2007 and for the IEEE Industry Applications Society from 2010 to 2011 as well as from 2017 to 2018. Between 2019 and 2020, he is the President of IEEE Power Electronics Society. He is the Vice-President of the Danish Academy of Technical Sciences. He has been nominated in 2014.2018 by Thomson Reuters to be between the 250 most cited researchers in engineering in the world.

Jens Bo Holm-Nielsen received the M.Sc. degree in agricultural systems, crops and soil science, from the KVL, Royal Veterinary and Agricultural University, Copenhagen, Denmark, in 1980 and the Ph.D degree in process analytical technologies for biogas systems from Aalborg University, Esbjerg, Denmark, in 2008.

He is currently working with the Department of Energy Technology, Aalborg University, Aalborg, Denmark, and is the Head of the Esbjerg Energy Section. On this research, activities established the Center for Bioenergy and Green Engineering in 2009 and serve as the Head of the research group. He has vast experience in the field of Biorefinery concepts and Biogas Production–Anaerobic Digestion and Implementation Projects of Bio-Energy Systems in Denmark with provinces and European states. He served as the technical advisory for many industries in this field. He has executed many large-scale European Union and United Nation Projects in research aspects of bioenergy, bio refinery processes, the full chain of biogas and green engineering. He has authored more than 300 scientific papers. He was a member on invitation with various capacities in the committee for over 500 various international conferences and organizer of international conferences, workshops and training programmes in Europe, Central Asia, and China. His research interests include renewable energy, sustainability, green jobs.

Farooque Azam received the bachelor's degree in computer science and engineering from Visvesvaraya Technological University, Belgaum, India, in 2011, the master's degree in computer science and engineering from Jawaharlal Nehru Technological University, Hyderabad, India, in 2013.

He was an Assistant Professor and Head with MIT, Purnea, India. He is currently with the School of Computing and Information Technology, REVA University, Bangalore, India. He has authored scientific papers in International Journals. His research interests include design and realization of optimization algorithms in various applications such as renewable energy.

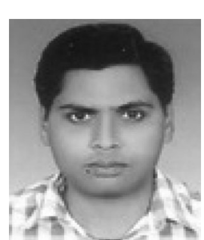

Amarjeet Kumar Sharma received the B.E. degree in electrical engineering from MIT Muzaffarpur, Muzaffarpur, India, in 2010, and the M.Tech. degree in electrical engineering (power system) from MAKAUT, Kolkata, India, in 2016.

He has authored and coauthored various papers in international journal and attended workshop/conferences on renewable energy and modern trends in electrical power system. His research interests include renewable energy and electrical machine. He is currently working as an Assistant Professor with the Department of Electrical Engineering, MIT Rambagh, Purnea (Bihar), India.